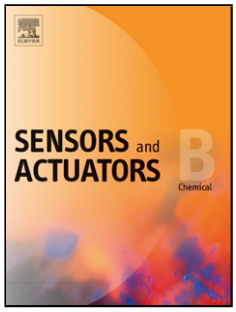

Title: TiO2:WO3 composite humidity sensors doped with ZnO and CuO investigated by Impedance Spectroscopy

Author: Pedro M. Faia Emanuel L. Jesus Cristina S. Louro

PII: S0925-4005(14)00806-5
DOI: http://dx.doi.org/doi:10.1016/j.snb.2014.06.117
Reference: SNB 17131

To appear in: *Sensors and Actuators B*

Received date: 17-3-2014
Revised date: 26-6-2014
Accepted date: 27-6-2014

Please cite this article as: P.M. Faia, E.L. Jesus, C.S. Louro, TiO2:WO3 composite humidity sensors doped with ZnO and CuO investigated by Impedance Spectroscopy, *Sensors and Actuators B: Chemical* (2014), http://dx.doi.org/10.1016/j.snb.2014.06.117

1. Introduction

The working principle of impedance ceramic metal oxide humidity sensor consists on the impedance changes that the sensing material experiments, when the sensor surface is exposed to a certain moisture concentration. Consequently, the performance of a ceramic sensor will be influenced by the porous microstructure and by the surface reactivity with the humidity: so if the sensitivity of these sensors depends on the microstructure, then the fabrication process becomes a strategic tool to improve the sensors response.

Relative Humidity (RH) is a parameter which can be used to specify moisture concentration (defined the ratio, at a given temperature, between the actual vapour pressure and the saturated vapour pressure). Various mechanisms have been proposed to explain the variations of electrical response and associated conduction mechanisms with humidity [1, 2]. Moseley *et al.* [3] have presented an extensive survey on the electrical behaviour of several semiconducting oxides, characterized their responses and proposed adequate interpretative models. The conduction mechanism can be either ionic either electronic type: in the ionic mechanism, the impedance of the sensor decreases with an increase of RH due to physisorption and capillary condensation of water molecules on the surface of the material [1]; in the electronic type, water molecules act as electron donors gas and chemisorption increases or decreases the electronic conductivity depending on whether the material is an n or p-type semiconductor [1]. In synthesis, electrical response of a porous ceramic, at different environmental humidity concentrations, is related to the water adsorption mechanism on the oxide surface [4, 5]. In our case, since WO_3 and TiO_2 are both n-type semiconductors, the sensitivity to humidity results mainly from electronic conduction with some ionic contribution. In the past, the authors studied the electrical response with humidity of a sensor with 48.92/51.08 volume percentage of TiO_2:WO_3, respectively, sintered in air at 700ºC [6]. That sensor exhibited almost linear response to humidity, see Figure 1: at a low operation frequency, impedance changes by more than two orders of magnitude, in the full RH range, suggesting good sensitivity to RH. In the literature there can be found references to works based on the use of the TiO_2:WO_3 pair for sensors fabrication: Xhu *et al.* [7] presented results for TiO_2:WO_3 nanocomposites response to benzene, while Chaudhari *et al.* [8] reported on the use of TiO_2:WO_3 nanocrystalline doped with a low concentration of Pt

for hydrogen sensing. More recently Zanetti *et al.* [9] studied the use of TiO_2: WO_3 nanopowders for humidity sensing, while varying WO_3 content.

Without any doubt, it is recognized by literature reports that if some of the positions initially occupied by the atoms of one of the metals are now occupied by atoms of another metal, material electrical response to humidity is altered (the electronegativity of the occupying metal atoms may be used to regulate the sensitivity). So doping a composite material with additional semiconducting metal oxides, will induce, in the final sensors structure, additional substitutions of metal atoms, from the initial composition, by metal atoms of the dopant, and consequently changes in the sensor electrical response to moisture will be observed.

In the present paper, authors report the specific behaviour found for composite sensors based on the TiO_2: WO_3 pair doped with CuO and ZnO. Sensors impedance dependency on RH, temperature and frequency is discussed, and a non-classical electrical model that applies to every sensor, for all relative humidity and temperature, is presented.

2. Electrical conduction and polarization due to water adsorption

Electrical conduction and polarization in a humidity sensor are prominently described in terms of the adsorbed water on the metal oxide surface but additionally by the capillary water that condensates within the pores [10, 11]: it should be stated that both these processes are favoured by the existence of a porous structure. Two types of water molecules adsorption take place: in the beginning chemisorption, followed by physisorption. The water vapour molecules are chemisorbed through a dissociative mechanism [12, 13]. For the case of TiO_2 and of WO_3, two surface hydroxyls per water molecule are formed: the hydroxyl group adsorbing on the surface metal ions and the proton forming a second hydroxyl with an adjacent surface O^{2-} ion [14]. On the other hand for CuO and for ZnO, only one hydroxyl group adsorbing on a surface metal ion, is formed.

Thus the initial chemisorbed layer is tightly attached to the surface grains. Once formed, which takes place for lower surface coverage's (around 20 to 30%), it is no further affected by exposure to humidity (desorption of the chemisorbed layer only takes by applying high temperatures to the metal oxide composite). As relative humidity (RH) increases, an additional layer of water molecules starts to be formed,

on the chemisorbed one. Many more physisorbed layers will be joined as humidity gets higher [15]. These layers are easily removed by decreasing the humidity. With more than one layer of physisorbed water molecules, water starts to condense into the capillary pores. The pore is filled or unfilled according to its radius and the thickness of the physisorbed layer, which depends on the magnitude of the relative humidity, in accordance to Kelvin equation [16].Typically, three regimes for the electrical conduction can be assumed [12,13, 17,18]: 1) with only a small coverage of water of the chemisorbed hydroxyl groups, proton H^+ hopping dominates; 2) with a fractional coverage of water, less than one physisorbed monolayer, hydronium H_3O^+ diffusion on hydroxyl groups dominates; 3) when water is abundant proton H^+ transfer process is dominant. Simultaneously, the sensor capacitance, due to electric polarization, is also conditioned by the movement of charges under the applied alternating electric field: in fact electric polarization is caused by the oscillation or reorientation of charges induced by the variation of the applied field. For the chemisorbed water molecules, as they are bound to the surface by two hydrogen bonds, they are not so free to reorient, following the external electric field, as those which are physisorbed, which are only singly bonded. Then the polarization, and consequently, the capacitance of the sensor will increase as less tightened are the water molecules with their neighbours, which happens as RH increases [19, 20]. Adding up to molecules orientation, there is also the contribution to the polarization due to mobile charges accumulated at the grain-grain barrier [17, 21].

In addition, the semiconducting character of our ceramic sensors, as also to be accounted for, in which the electrical conduction takes place through electron and hole transport from one grain to the next, over grain-grain barrier. The semiconducting behaviour can be described in terms of the band-like theory. For an n-type semiconducting sensor exposed to rising humidity concentration, the impedance decreases due to the above referred conduction modes: proton hopping, electronic and ionic diffusion and transport mechanisms and polarisation mechanisms.

3. Experimental

The bulk sensors were fabricated from as received TiO_2, WO_3, CuO and ZnO dry-powders from FLUKA, all with a purity of 99% and a medium grain size lower than 45

nm. First, the TiO_2 and the WO_3 powders were mixed in the mole volume ratio percentages of 48.92:51.08%. Then similar mole volume ratio percentages of ZnO and CuO, 7% in the present case, were added to form Sensor A and sensor B, respectively (two of each designated type of sensors were produced and later characterised morphologically and electrically). After they were moulded (mould dimensions: 8 mm long, 6 mm wide and 1 mm height) the sensors were successively subjected to uniaxial and isostatic pressing, at the pressures of 10 MPa and 200 MPa, respectively. The green samples were then sintered in air for 120 minutes at the temperature of 700ºC, with rising and falling temperatures rates of 20 ºC/min approximately.

The phase composition of both sensors was examined using the X-Ray Diffraction (XRD) on a Philips X'Pert, PW 3040/00, diffractometer. The measurements were performed by the Bragg-Brentano method using Co radiation (K_α=1. 78897 Å) in angle 2θ interval from 20 to 60 degrees with a step of 0.04 degrees and a scanning time of 0.5 sec in point.

Porosity distribution analysis of the sensors, based on the intrusion/extrusion curves, were performed using a Micrometrics porosity meter, model Poresizer 9320, starting with sensors degasification, followed by mercury intrusion pressured analysis starting at 0.5 up to 30000 Psia. The sensors microstructure was characterised using a Philips Scanning Electron Microscope (SEM), model XL 30 TMP, operated at 30 kV.

The electrical characterisation of the sensors was performed in a chamber, with a volume of approximately 6.5 litters, the temperature of which was electronically controlled better than 1ºC in different constant atmospheres with constant relative humidity (RH) varying from 5% to 35%, with increments of 5%, and then from 40% to 90%, with increments of 10%. The sensors were tested for the different prepared mixtures, at the temperatures of 30 and 40ºC. The different relative humidities were obtained by mixing, in the chosen ratio, water saturated air, obtained by bubbling synthetic air through water in a bubbler, with dry synthetic air. Volumetric flow rates of both saturated wet and dry air were controlled by independent mass flow controllers, and then joined together in a mixer before passing tangentially over the surface of the sensors placed inside the test chamber. All the electrical measurements were performed with the samples submitted to a 5 l/h flow of a given mixture kept for at least 90 minutes, at a constant temperature. For that purpose, a pair of gold

electrodes was chemically evaporated through a mask onto the surface of each sensor, and heated afterwards up to 700ºC, for 15 minutes. The dependence of the electrical impedance of the samples on temperature and RH was investigated using complex impedance spectroscopy. Impedance spectra were obtained in the range 100 Hz to 10 MHz, with a peak voltage of 0.5 V, by means of an Impedance/Gain-Phase analyser from Hewlett-Packard (model HP4294A).

4. Results and Discussion

4.1. Microstructure

As already stated for each type of TiO_2: WO_3 doped sensors, two samples were prepared and characterised: the ones designated as sensor A, were doped with ZnO and the ones designated as sensor B, were doped with CuO. The morphological data here presented and discussed reflect the observations for both sensors of each composition which were very similar, and so only one of each type is reproduced.

Concerning the structural characterization of sensors, the XRD diffraction patterns are presented in Figure 2. As can be concluded the sensors present different phases arrangements. As can be concluded, both sensors present the rutile TiO_2 phase. These results are in agreement with previous studies [22, 23] showing a typically anatase to rutile transformation of the ceramic after sintering. Nevertheless the final structure of both sensors depends on the nature of the dopant. Doping with CuO leads to the formation of a new phase, the copper tungstate $CuWO_4$, during sintering. This result confirms the low solubility of both WO_3 and CuO into TiO_2 based materials [24]. The addition of Zn (2+) through the use of ZnO additive marked enhancement the anatase to rutile transformation, sensor A. As reported elsewhere the substitution of Ti by lower valence Zn result of an increased of oxygen vacancies [25] reducing the lattice constraint and facilitates the reconstructive phase transformation of titania.

The pore size distribution curves, obtained by the mercury intrusion method, are presented in Figure 3. For sensor A, a bimodal distribution is visible: a first region suitable for capillary condensation, between 0.3 and 0.1 μm, a second above 2 μm: nevertheless in the latter mentioned region, it should be mentioned that it could be split in two dominant areas, the first containing the pores between, 1.5 and 13 μm and the second containing the pores above 100 μm. For sensor B a trimodal

distribution is observed: a first region suitable for capillary condensation, between 0.5 and 0.2 μm, a second one between 13 and 2 μm, and the last one above 100 μm. Typically, the pores with size above 100 μm simply serve as passage for the water vapour, and capillary condensation of water vapour majorly occurs in the mesopore range. Comparing both sensors porosimetry, the main differences arise from the region concerning pores below 1 μm: sensor A, exhibits a much larger contribution of pores in that region, which are additionally lower in dimension, when compared with the ones present in sensor B.

SEM micrographs of the both sensors are presented in Figure 4. While For sensor A large agglomerates of quasi-spherical grains, of average dimensions around 100-300 nm are visible, in sensor B not only some small agglomerates of quasi-spherical grains are visible (grains which exhibit an average dimension lower than 400-100 nm), as also some cylindrical shaped grains of reaching more that 1μm in length are present.

In resume both X-ray diffraction, porosimetry and SEM allowed to observe that there are major structural differences between both type of sensors: the change in the dopant clearly introduces changes between sensors A and B observable morphology, which will much probably induce differences in sensors electrical response to moisture.

4.2. Recorded spectra of the sensors and interpretation

As already stated for each type of TiO_2; WO_3 doped sensors, two samples were prepared and tested (the ones designated as sensor A, doped with ZnO and the ones designated as sensor B, doped CuO) and the data here presented and discussed reflect the observations for both sensors of each composition (in all the graphs, the data showed are for each point the average value of all the sets of measures taken for both sensors of each composition).

Since the first work by Bauerle [26], complex impedance spectroscopy has been largely used to characterise electrical response of ceramics [27]. In Figures 5 through to 7, Nyquist plots obtained for both doped sensors, at 30 and 40ºC, for the full tested RH range, are shown. Complex impedance data integrity validation was ensured by the Hewlett-Packard equipment, once it has inbuilt Kramer-Krönig transformations. As explained in the previous section, water molecules start to be adsorbed on the surface via a dissociative chemisorption process. Electrons are accumulated at the

sensor surface and consequently, the resistance of the sensing element decreases with RH increase. As water layers continue to be formed on the material surface, the activation energy decreases and ions start to participate in the conduction as carriers. With the increase of water layers pores start to get filled, and protons can then hop between adjacent water molecules via a Grotthuss chain reaction.

The impedance spectra illuminate the different phenomena of electrical conduction and polarization that occur in these materials in the presence of water molecules. A semicircle is typical of a relaxation mechanism. In our case there are contributions of the interaction of water molecules with the grains and grain boundaries at the surface [6, 28]. A straight line is due to electrical diffusion. In our case, diffusion seems also to be present in the overall electrical, particularly for the ZnO doped sensor, and more than one contribution can be assumed: one from the layer deposited on the surface, another from the water enclosed inside the pores, and one last one from the interface between the water and the electrodes.

For both sensors, and at all the tested temperatures, the impedance area under the Nyquist plots decreases with the increase of RH.The described behaviour, observed in Figures 5, 6 and 7, and regarding the overall sensor impedance, which diminishes with RH increase, is confirmed by looking at Figure 8, where the modulus of the sensor A impedance, at 100 Hz and 1 kHz, for all the test temperatures and for the full RH range is represented, and at Figure 9, where the sensor B impedance modulus are compared for the full RH range, at the temperatures of 30, and 40ºC and at the frequencies of 1 kHz and 10 kHz.

Also by looking at figures 5 through 7 two additional and relevant evidences must be pointed out: 1) as mentioned earlier, for sensor A a straight line seems to be present at the lower frequencies in the lower RH range, confirming the contribution of diffusion mechanisms to the overall electrical response of this sensor, see figures 5 and 6; 2) for sensor B, a “switch” type behaviour seems to be dominant: in fact not only this sensor shows lower sensitivity to moisture, when compared with sensor A, in the lower RH range, as also an abrupt change of the overall sensor impedance is observed, when RH is raised from 30 to 35%. Besides, as RH is further increased above 35% sensor B impedance stays almost unchangeable.

Authors, however, are not totally surprised with the evidences above described: as anticipated, and in accordance with the differences found in the sensors structure, the impedance spectra have very different shape and visible contributions. Moreover,

the reasons for the differences are, in the authors opinion, totally connected with the differences in the sensors structure: a larger number of capillary pores favour the moisture sensitivity, which is the case of sensor A, and not the case of sensor B, so, when only a small quantity of capillary pores is available, as soon as they are all filled with water, no longer the sensor electrical response, as is the case for sensor B, is affected by moisture concentration increment. Authors also believe that the sudden change in the overall impedance of this sensor which is observable when RH is raised from 30 to 35% might be connected to the a rapid change in diffusion contribution that takes place inside the pores that get filled with water: at the beginning, and for the smaller water coverage rations, a possible small contribution can be assumed, which suddenly and as the pores get entirely filled, seems to negligible. Besides, sensor B X-ray diffraction showed the presence of a $CuWO_4$ phase after sintering, know to exhibit a greater chemical stability (not only in this compound the 2p-band is far below the Fermi energy, and consequently its contribution to conduction at low temperature seems negligible as in transition metal compounds the mobility of charge carriers is very low at low temperature due to the narrowness of the d-band [29]), which also contributes to the observed overall electrical response and reduced sensitivity to moisture changes, when compared with sensor A.

Both sensors present sensitivity to humidity changes. The ZnO doped sensor, in particular, exhibits sensitivity in the entire RH range: however, when compared with the undoped sensor (figure 1), the overall sensitivity is lower (only around one order of magnitude variation, while the undoped one, presented almost 3 orders of magnitude). By the contrary, the CuO doped sensor, sensor B, only exhibits some sensitivity in the lower humidity range, and even lower than the shown by sensor A: besides, it's operation is more similar to a switch which threshold corresponds to the change between the lower and higher humidity range, and takes place around 30% RH.

Nevertheless, and generally speaking, both sensors impedance decrease, when submitted to an RH increase from 10 up to 90%, which is typical of an n-type behaviour and, as the authors assume, due to a decrease of the band bending. The band bending is due to the already referred conduction modes: proton hopping, electronic and ionic diffusion and transport mechanisms and polarisation mechanisms. Nevertheless, and as assumed previously by the authors, sensors

electrical response to moisture are well differenced and in accordance with the variances documented for their respective structure, in direct relation with the dopant used.

4.3. Electrical circuit model of the sensors

AC equivalent circuits for humidity sensors, which represent the effect of moisture on the electrical conduction and polarization of the material, have been proposed by several authors [27, 31, 32]. In general, for a given data set, there exists more than one equivalent circuit which gives a reasonable fitting. The choice between these circuits has to be based both in simplicity and consistency with the known physical and chemical processes which take place in the system [26]. Typically, the different mechanisms contributing to a sensor overall electrical response to moisture, are accepted to be modelled by a serial association of a set of smaller circuits, each one representing a particular contribution/effect, see Figure 10.

However authors believe that, since the different phenomena know to be present with our sensors, and consequently the diverse electrical conduction mechanisms contributing to the overall electrical response, arise from diverse locals of the sensor structure which take place simultaneously, i.e., in parallel, a different approach might be taken. So, instead of the traditional serial model circuit, a parallel one is being tested, see Figure 11.

With this approach authors believe that a more suitable match between the physical and chemical reactions that take place at each instant, observable by looking at the electrical response of the sensor, which is the sum of several contributions, and the equivalent model circuit, is achieved. In fact, if some contribution for the overall electrical response of the sensor is not present for some humidity range, which would then be represented by an open circuit equivalence, in the case of the electrical model circuit where all contributions are serial connected, an open circuit situation would be created, originating an overall model circuit impedance of infinite value, which would be absolutely mean less and unreal. By the contrary, if the contributions are connected in parallel, the non-existence of a certain contribution will not create the same type of contradiction: in reality, an open circuit situation due to a non-existent contribution for a certain RH range, does not create any ambiguous form of the equivalent model circuit, simply because it just not contributes as the remaining ones still due, due to the parallel connection.

All the obtained complex impedance plots were modelled by the equivalent circuit shown in Figure 11. C_{geo} represents the geometrical capacitance (contribution of the bulk properties), the parallel R_1//C_1represents the bulky granular contribution and the parallel R_2 // C_2 the grain boundary contribution for the overall sensor conduction process: let's recall that for a general R//C circuit it's impedance is given by

$$Z_{R//C} = \frac{R}{1+w^2C^2R^2} - j\frac{wCR}{1+w^2C^2R^2}) \qquad (1)$$

Charge diffusion through the adsorbed water, enlarged by the contributions of capillary pores and other inhomogeneity's, is represented by a Constant Phase Element, CPE, described by [33]

$$(Z_{CPE} = A^{-1}w^{-n}\left(\cos n\pi/2 - j\sin n\pi/2\right) \qquad (2)$$

In fact in the filled pores, the mechanism is under diffusion control, as it is assumed that the kinetics of the charge transfer at the water surface layer-filled pores interfaces is much faster than the diffusion of H_3O^+ ions inside the pores [33]. Surface roughness has also been considered as an important contributing factor [34]. Another diffusion contribution also takes place on the electrodes, when they become covered by water.

For both above referred diffusion mechanisms, the interfacial character of their impedance makes it partly capacitive as well resistive in nature. CPE_{po} has to do with the contribution of the pores, due to diffusion phenomena taking place inside the water filled pores, and CPE_{el} is related to the electrodes-water layer interface diffusion phenomena that take place at that interface. Both of them contribute to the overall conduction changes observed in the sensors.

However, for the case of the sensors doped with CuO the grain and grain boundary contributions seem to be the dominant conduction mechanisms: truly and by looking at the Nyquist plots, no straight line is apparently observable, which are typical of the diffusion mechanisms. That does not mean that they are not present at all, only that there contribution is not the dominant one.

In Figures 12 and 13 are represented examples of obtained impedance spectra and their respective fit curves, for both sensors and diverse RH and working temperatures, T: the superposition between experimental and simulation curves is quite good, which confirm the usability and validity of chosen electrical circuit model under this new approach.

In tables 1 and 2 are the best fit parameters for the new proposed electrical equivalent circuit, corresponding to the experimental fitted Nyquist plots presented in figures 12 and 13, which were reached after several attempts. In those tables A_{el} and n_{el} represent the two parameters of the impedance CPE_{el}, while A_{po} and n_{po} represent the two parameters of the impedance CPE_{po}, both described using equation (2). In those fitted parameters, it can also be observed the differences between the sensors electrical response contributions that are present, according to the author's opinion.

In fact for sensor A, parameters reflect the contribution of not only the grains and grain boundaries, as also the ones originated by diffusion in the pores that get filled with water and by diffusion on the electrodes interfaces that get covered by water: the overall of the last two referred contributions, both decrease with RH increase, reflecting the observation previously reported by the authors, in which and at low RH, in the Nyquist plots for this sensor a straight line was visible, while for higher RH humidity's they become less relevant to the overall sensor electrical response, once it is no longer visible in the plots.

By the contrary for sensor B, no evident diffusion contributions seem to be present, since no straight line is visible in the Nyquist plots: and once again the parameters reflect that, since the diffusion contribution due to the pores that get filled with water is very low, when compared with the observed for sensor A, while the diffusion contribution from the electrodes interface that get covered with water is almost unchangeable. Authors however are aware that further simulation work as still to be done with other sensors and respective Nyquist plots before making general use of this type of model circuit.

5. Conclusions

The $TiO_2:WO_3$ composites sensors, with 48.92/51.08 respective volume percentages, doped with ZnO (sensor A) and with CuO (sensor B) were prepared by a classical route, at a sintering temperature of 700ºC. The obtained experimental results confirm that doping is a way of changing materials overall electrical response The complex impedance was measured at different RHs, in the range of 5% - 90%. Both sensors exhibit sensitivity to RH, particularly sensor A, however lower than the previously reported for the undoped sensor: a different dopant proportion might present enhanced sensitivity. By the contrary, sensor B, presents only RH sensitivity in the lower RH range: besides is behaviour is more similar to a switch, when alternating

humidity operation interval between low and high range. Diverse transport mechanisms, such as electron conduction, ion diffusion and proton hopping, contribute to the sensors electrical response to RH. A non-traditional equivalent electrical circuit, modelling the sensors response to RH, is presented which allows to better understand the diverse charge transport mechanisms and their relation with sensors morphology.

Acknowledgments

This research is sponsored by FEDER funds, through the program COMPETE – Programa Operacional Factores de Competitividade –, and by national funds, through FCT – Fundação para a Ciência e a Tecnologia –, under the project PEst-C/EME/UI0285/2013.

Biographies

Pedro M. Faia received his degree in Electrical Engineering (1990), his Master of Science in Automation (1994) and a Ph.D in Electronic Materials (2003), all from the University of Coimbra. He is actually an Auxiliary Professor at the Department of Electrical Engineering and Computers of the University of Coimbra where is research interests concern the research and development of solid state chemical sensors, sensor integration techniques, Electrochemical sensor and biosensors, Impedance Spectroscopy technique and applications. He is a member of the Portuguese Materials Society.

Emanuel Ladeiro de Jesus received is Master of Science in Electrical Engineering in 2013, from the University of Coimbra. He is actually working in Executive Help - Industrial Laboratory and is scientific interest's concern sensors calibration and data measurement techniques.

Cristina Santos Louro graduated in Chemical Engineering at the Faculty of Science and Technology, University of Coimbra (FCTUC, 1991). The Master Science Degree in Materials Engineering (FCTUC) was achieved in 1995 and the Ph.D was attained in 2000 (FCTUC) in Mechanical Engineering field. Actually, she holds the permanent position of Auxiliary Professor in the Mechanical Engineering Department - Coimbra University. Her research interests cover areas such Hard Coatings, sputtering production, optimization and characterization, for mechanical, biomedical and nuclear applications; and Advanced Ceramics, chemical modification, processing and microstructural control, for humidity sensors and armour protection. She is an effective member of the Surface Engineering Group, a sub-group of the Centro de Engenharia Mecânica da Universidade de Coimbra (CEMUC).

References

[1] E. Traversa, A. Bearzotti, A novel humidity-detection mechanism for ZnO dense pellets, Sens. Actuators B 23 (1995) 181-186.

[2] N. Yamazoe, Y. Shimizu, Humidity sensors: principles and applications, Sens. Actuators 10 (1986) 379-398.

[3] P.T. Moseley, A.M. Stoneham, D.E. Williams, Techniques and Mechanisms in Gas sensing, Adam Hilger, Bristol/New York, 1991, pp.108-138.

[4] E. McCafferty, A.C. Zettlemoyer, Adsorption of water vapour on Fe_2O_3, Discuss. Faraday Soc. 52 (1971) 239-263.

[5] M.T. Wu, H.T. Sun, L. Ping, CuO-doped $ZnCr_2O$-$_4$-$LiZnVO_4$ thick-film humidity sensor, Sens. Actuators 17 (1994) 109-112.

[6] P.M. Faia, A.R. Ferreira, C.S. Furtado, Establishing and interpreting an electrical circuit representing a TiO_2-WO_3 series of humidity thick film sensors, Sens. Actuators B 140 (2009) 128-133.

[7] Y. Zhu, X. i Su, C. Yang, X. Gao, F. Xiao, J. Wang, Synthesis of TiO_2–WO_3 nanocomposites as highly sensitive benzene sensors and high efficiency adsorbents, J. Mater. Chem., 22 (2012), 13914-13917.

[8] G.N. Chaudhari, A.M. Bende, A.B. Bodade, S.S. Patil, V.S. Sapkal, Structural and gas sensing properties of nanocrystalline TiO2:WO3-based hydrogen sensors, Sens. Actuators B, 115 (2006), 297-302.

[9] S.M. Zanetti, K.O. Rocha, J.A.J. Rodrigues, E. Longo, Soft-chemical synthesis, characterization and humidity sensing behavior of WO_3/TiO_2 nanopowders, Sens. Actuators B 190 (2014), 40-47.

[10] B.M. Kulwicki, Ceramic sensors and transducers, J. Phys. Chem. Solids 45 (1984) 1015-1031.

[11] B.M. Kulwicky, Humidity Sensors, J. Am. Ceram. Soc. 74 (1991) 697-708.

[12] J.H. Anderson, G.A. Parks, The Electrical Conductivity of Silica Gel in the Presence of Adsorbed Water, J. Phys. Chem. 72 (1968) 3362-3368.

[13] J.J. Fripiat, A. Jelli, G. Poncelet, J. André, Thermodynamic Properties of Adsorbed Water Molecules and Electrical Conduction in Montmorillonites and Silicas, J. Phys. Chem. 69 (1965) 2185-2197.

[14] W. Ku, J.U. Meyer, A novel thick-film ceramic humidity sensor, Sens. Actuators B, 40 (1997), pp. 175–182.

[15] W.M. Sears, The effect of oxygen stoichiometry on the humidity sensing characteristics of bismuth iron molybdate, Sens. Actuators B 67 (2000) 161-172.

[16] P.M. Faia, A.R. Ferreira, C.S. Furtado, AC impedance spectroscopy: a new equivalent circuit for titania thick film humidity sensors, Sens. Actuators B 107 (2005) 353-359.

[17] T. Morimoto, M. Nagao, F. Tokuda, The relation between the amounts of chemisorbed water in metal oxides, J. Phys. Chem. 73 (1969) 243-248.

[18] J. Holc, J. Slunčko, M. Hrovat, Temperature characteristics of electrical properties of (Ba, Sr)TiO_3 thick film humidity sensors, Sens. Actuators B 26-27 (1995) 99-102.

[19] M.G. Baldwin, J.C. Morrow, Dielectric Behaviour of Water Adsorbed on Alumina, J. Chem. Phys. 36 (1962) 1591-1593.

[20] K.S. Cole, R.H. Cole, Dispersion and Absorption in Dielectrics. I. Alternating Current Characteristics, J. Chem. Phys. 9 (1941) 341-351.

[21] T. Morimoto, T. Iwaki, Dielectric Behaviour of Adsorbed Water – Part 1, J. Chem. Soc., Faraday Trans. 1 83 (1987) 943-956.

[22] X.Z. Ding, X.H. Liu, Y.Z. He, Grain size dependence of anatase-to-rutile structural transformation in gel-derived nanocrystalline titania powders, J. of Mater. Science Letters, 15 (1996) 1789-1791.

[23] S. Vargas, R. Arroyo, E. Haro, R. Rodriguez, Effects of Cationic Dopants on the Phase Transition Temperatures of Titania Prepared by the Sol-Gel Method, J. Mater. Res., 14 (1999) 3932-3937.

[24] S. Ma, P.R. Cantwell, T.J. Pennycook, N. Zhou, M.P. Oxley, D.N. Leonard, S.J. Pennycook, J. Luo, M.P. HarmerGrain boundary complexion transitions in WO_3- and CuO-doped TiO_2 bicrystals, Acta Materialia 61 (2013) 1691-1704.

[25] M. Inagaki, Y. Nakazawa, M. Hirano, Y. Kobayashi, M. Toyoda , Preparation of Stable Anatase-Type TiO_2 and Its Photocatalytic PerformanceInt. J. Inorg. Mater. 3 (2001) 809-811.

[26] J.E. Bauerle, Study of Solid Electrolyte Polarization by a Complex Admittance Method, J. Phys. Chem. Solids 30 (1969) 2657-2670.

[27] J.R. MacDonald, Impedance Spectroscopy, John Wiley & Sons, New York, 1987.

[28] G. Gusmano, A. Bianco, G. Montesperelli and E, Traversa, An EIS study of the humidity-sensitive electrical conduction of alkali-doped TiO_2 films, Electrochim. Acta 41 (1996) 1359-1368.

[29] R Bharati, R Shanker and R A Singh Pramana, Electrical transport properties of $CuWO_4$, Journal of Physics 14 6 (1980) 449-454,

[30]: Ch. Ziegler, W. Göpel, H. Hämmerle, H. Hatt, G. Jung, L. Laxhuber, H. Schmidt, S. Schütz, F. Vögtle and A. Zell, Bioelectronic noses: a status report. Part II, Biosensors and Bioelectronics, a998, pp 539-571.

[31] S. Agarwal, G.L. Sharma, Humidity sensing properties of (Ba, Sr) TiO_3 thin films grown by hydrothermal-electrochemical method, Sens. Actuators B 85 (2002) 205-211.

[32] G. Gusmano, G. Montesperelli, P.Nunziante, E. Traversa, Study of the conduction mechanism of $MgAl_2O_4$ at different environmental humidities, Electrochim. Acta 38 (1993) 2617-2621.

[33] M. Su, J. Wang, H. Du, P. Yao, Y. Zheng, X. Li, Characterization and humidity sensitivity of electrospun ZrO_2:TiO_2 hetero-nanofibers with double jets, Sens. Actuators B, 161 (2012) 1038-1045.

[34] S.-H. Song, X. Wang, P. Xiao, Effect of microstructural features on the electrical properties of TiO_2, Mater. Sci. Eng., B 94 (2002) 40-47.

Table 1 – fit parameters for presented Nyquist plots of sensor A

RH(%) / T(ºC)	R_1 (Ω)	C_1 (F)	R_2 (Ω)	C_2 (F)	C_{geo} (F)	A_{el} (Ω^{-1})	n_{el}	A_{po} (Ω^{-1})	n_{po}
80 / 30	$4.49E^{+5}$	$1.10E^{-10}$	$5.15E^{+5}$	$4.84E^{-12}$	$5.18E^{-13}$	$1.24E^{-9}$	$9.74E^{-1}$	$2.46E^{-8}$	$3.95E^{-1}$
30 / 30	$2.22E^{+6}$	$2.82E^{-12}$	$1.00E^{+6}$	$2.78E^{-11}$	$4.52E^{-12}$	$2.78E^{-8}$	$3.23E^{-1}$	$1.99E^{-9}$	1
20 / 40	$3.00E^{+6}$	9.79E-^{12}	$8.00E^{+5}$	$2.83E^{-12}$	$3.17E^{-12}$	$3.28E^{-7}$	$8.79E^{-3}$	$2.57E^{-11}$	1

Table 2 – fit parameters for presented Nyquist plots of sensor B

RH(%) / T(ºC)	R_1 (Ω)	C_1 (F)	R_2 (Ω)	C_2 (F)	C_{geo} (F)	A_{el} (Ω^{-1})	n_{el}	A_{po} (Ω^{-1})	n_{po}
80 / 30	$1.48E^{+4}$	$1.11E^{-11}$	$1.24E^{+3}$	$6.22E^{-11}$	$3.92E^{-12}$	$3.52E^{-9}$	$5.96E^{-1}$	$5.53E^{-5}$	$9.04E^{-3}$
30 / 30	$1.41E^{+3}$	$2.60E^{-12}$	$3.13E^{+4}$	$6.79E^{-12}$	$1.18E^{-12}$	$1.41E^{-9}$	$6.64E^{-1}$	$1.50E^{-5}$	$1.19E^{-1}$
20 / 40	$1.63E^{+3}$	$2.08E^{-9}$	$2.91E^{+4}$	$1.09E^{-12}$	$1.09E^{-12}$	$3.33E^{-10}$	$7.89E^{-1}$	$1.39E^{-4}$	$7.13E^{-1}$

Figure 1 - Humidity electrical response of an Ti/W composite oxide bulk sensor at 25ºC (48.92 and 51.08% (w/w) of Ti and of W atoms): i) and ii) Nyquist plot (red, green, dark blue, orange, rose, brown light blue, stand for 15, 32, 36, 43, 66, 92 and 100% RH); iii) and iv) Impedance modulus at 100Hz and 1kHz, respectively (adapted from [6]).

Figure 2 - X- ray diffraction patterns of sensors: i) sensor A (TiO_2-WO_3 doped with ZnO); ii) sensor B (TiO_2-WO_3 doped with CuO).

Figure 3 - Log differential intrusion as a function of pore diameter: for both sensors A and B (sensor A – blue. Sensor B - brown): i) micro pores range; ii) nano pores range.

Figure 4 - SEM microscopies: i) ZnO doped sensor; ii) CuO doped sensor.

Figure 5 - Nyquist plot for sensor A at 30ºC, in the lower and higher humidity range, i) and ii) respectively (dark blue, black, orange, dark green, brown, rose, purple, grey, red, and light blue, and light green stand for 10, 20, 30, 40, 50, 60, 70, 80 and 90% RH, in turn).

Figure 6 - Nyquist plot for sensor A at 40ºC, in the lower and higher humidity range, i) and ii) respectively (dark blue, black, orange, dark green, brown, rose, purple, grey, red, and light blue, and light green stand for 10, 20, 30, 40, 50, 60, 70, 80 and 90% RH, in turn).

Figure 7 - Nyquist plot for sensor b at 30 and 40ºC, i) and ii) respectively (dark blue, black, orange, dark green, brown, rose, purple, grey, red and light blue, stand for 5, 15, 25, 30, 35, 40, 50, 70, 80 and 90% RH, in turn).

Figure 8 - Impedance change with RH, at 100 and 1 kHz, for sensor A, i) and ii), respectively, for all test temperatures (red 30ºC and blue 40ºC).

Figure 9 - Impedance change with RH, at 100 and 1 kHz, for sensor B, i) and ii), respectively, for all test temperatures (red 30ºC and blue 40ºC).

Figure 10 - Typical approach for modelling sensors electrical response to gases using model circuits (adapted from [30])

Figure 11 - Current equivalent circuit for the sensors.

Figure 12 - Nyquist plots and best fitting for Sensor A, at 30ºC and 80% RH, at 30ºC and 30% RH and at 40ºC and 20% RH respectively i), ii), and iii) (red obtained spectra, blue fitted spectra).

Figure 13 - Nyquist plots and best fitting for Sensor B, at 30ºC and 80% RH, at 30ºC and 30% RH and at 40ºC and 20% RH respectively i), ii), and iii) (red obtained spectra, blue fitted spectra).

Figure 1 - Humidity electrical response of an Ti/W composite oxide bulk sensor at 25ºC (48.92 and 51.08% (w/w) of Ti and of W atoms): i) and ii) Nyquist plot (red, green, dark blue, orange, rose, brown light blue, stand for 15, 32, 36, 43, 66, 92 and 100% RH); iii) and iv) Impedance modulus at 100Hz and 1kHz, respectively (adapted from [6]).

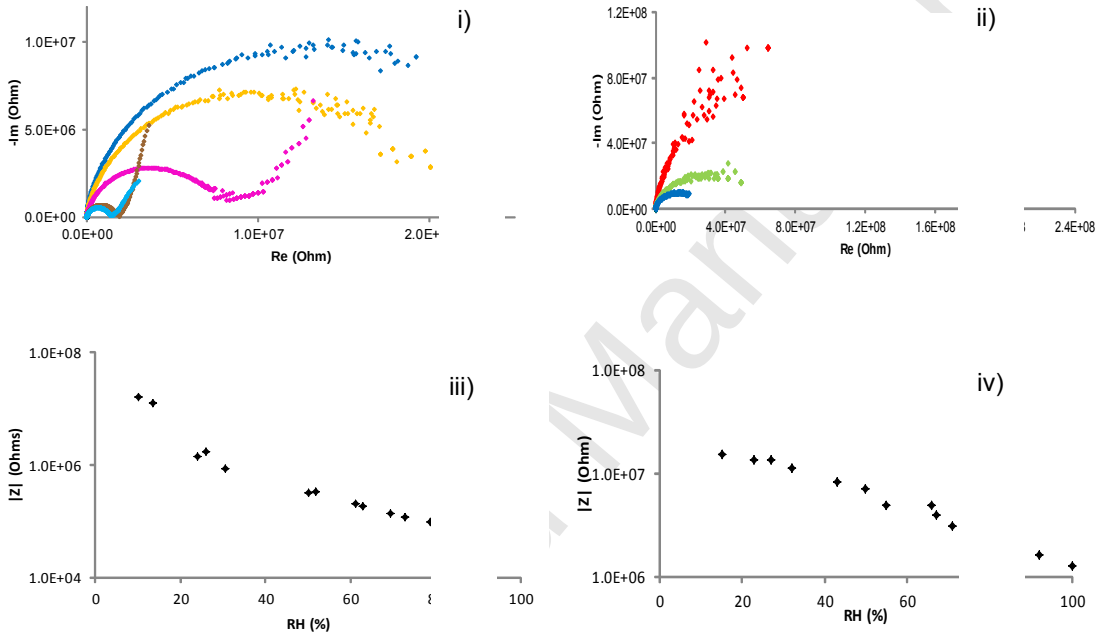

Figure 2 - X- ray diffraction patterns of sensors: i) sensor A (TiO_2-WO_3 doped with ZnO); ii) sensor B (TiO_2-WO_3 doped with CuO).

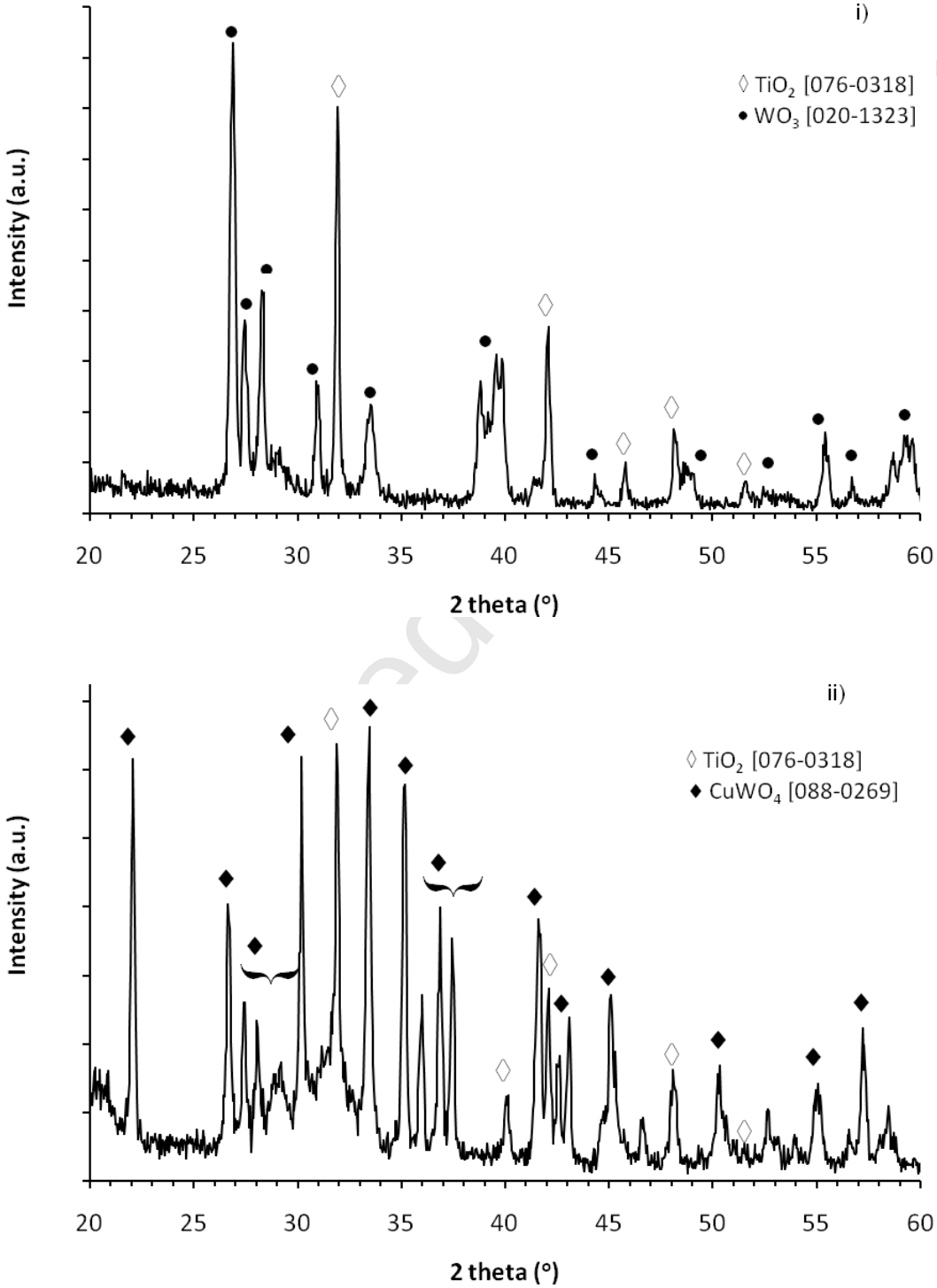

Figure 3 - Log differential intrusion as a function of pore diameter: for both sensors A and B (sensor A – blue. Sensor B - brown): i) micro pores range; ii) nano pores range.

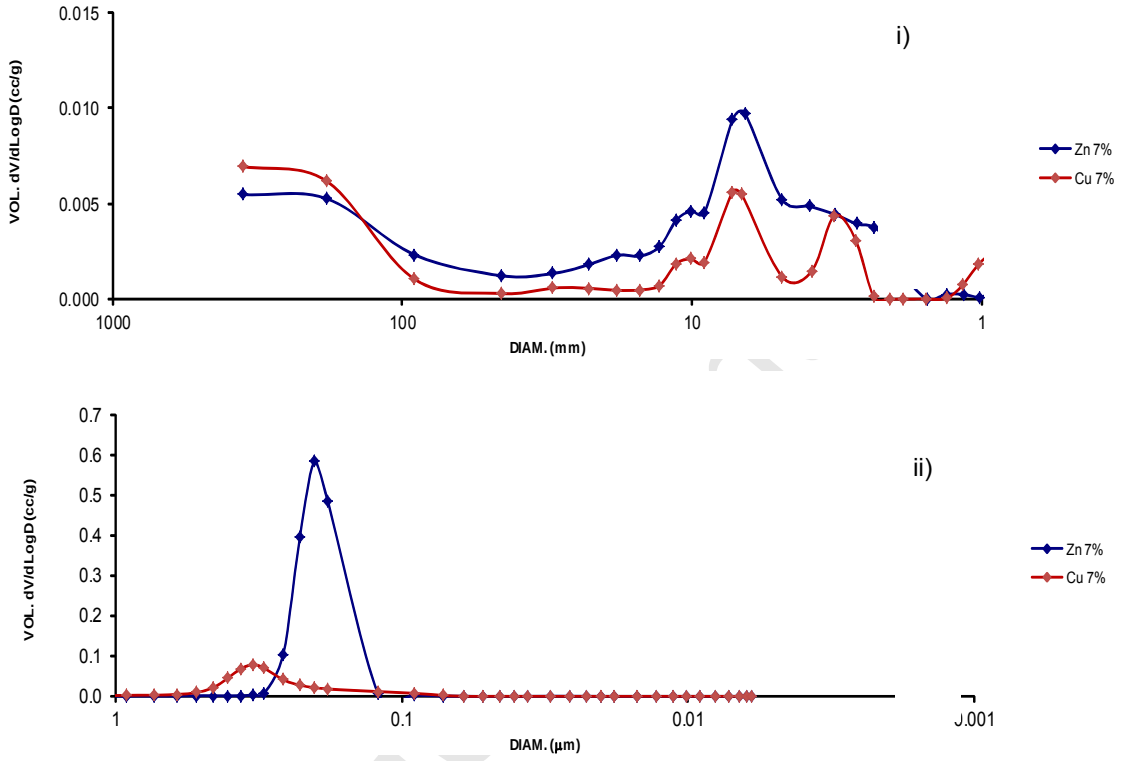

Figure 4 - SEM microscopies: i) ZnO doped sensor; ii) CuO doped sensor.

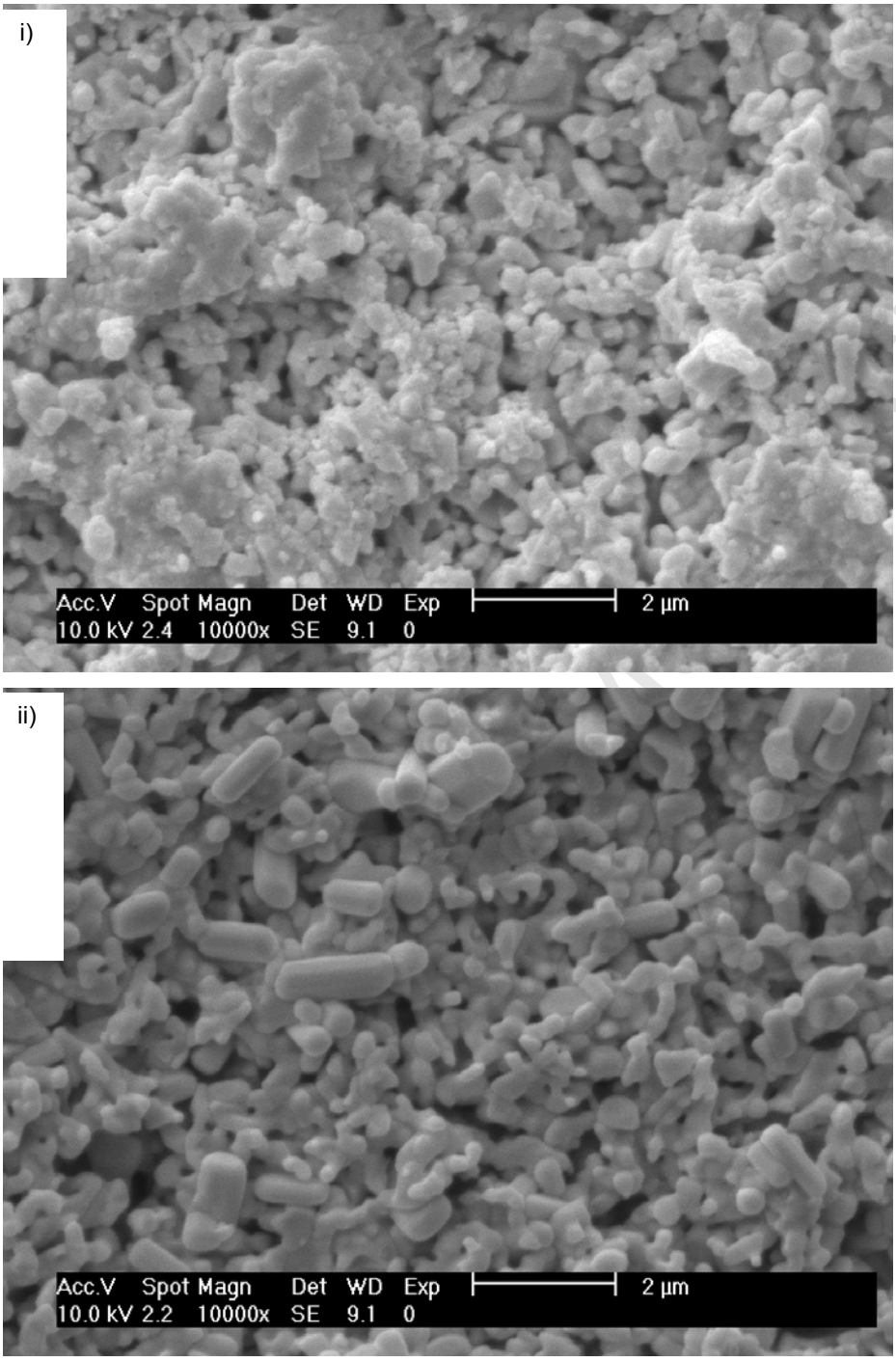

Figure 5 - Nyquist plot for sensor A at 30ºC, in the lower and higher humidity range, i) and ii) respectively (dark blue, black, orange, dark green, brown, rose, purple, grey, red, and light blue, and light green stand for 10, 20, 30, 40, 50, 60, 70, 80 and 90% RH, in turn).

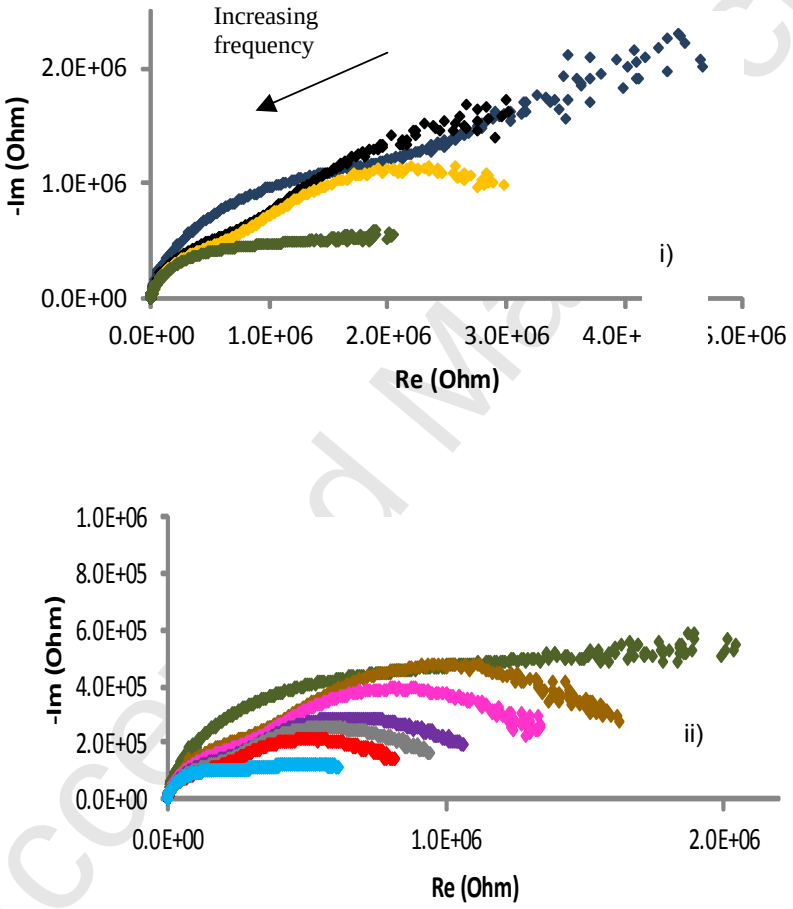

Figure 6 - Nyquist plot for sensor A at 40ºC, in the lower and higher humidity range, i) and ii) respectively (dark blue, black, orange, dark green, brown, rose, purple, grey, red, and light blue, and light green stand for 10, 20, 30, 40, 50, 60, 70, 80 and 90% RH, in turn).

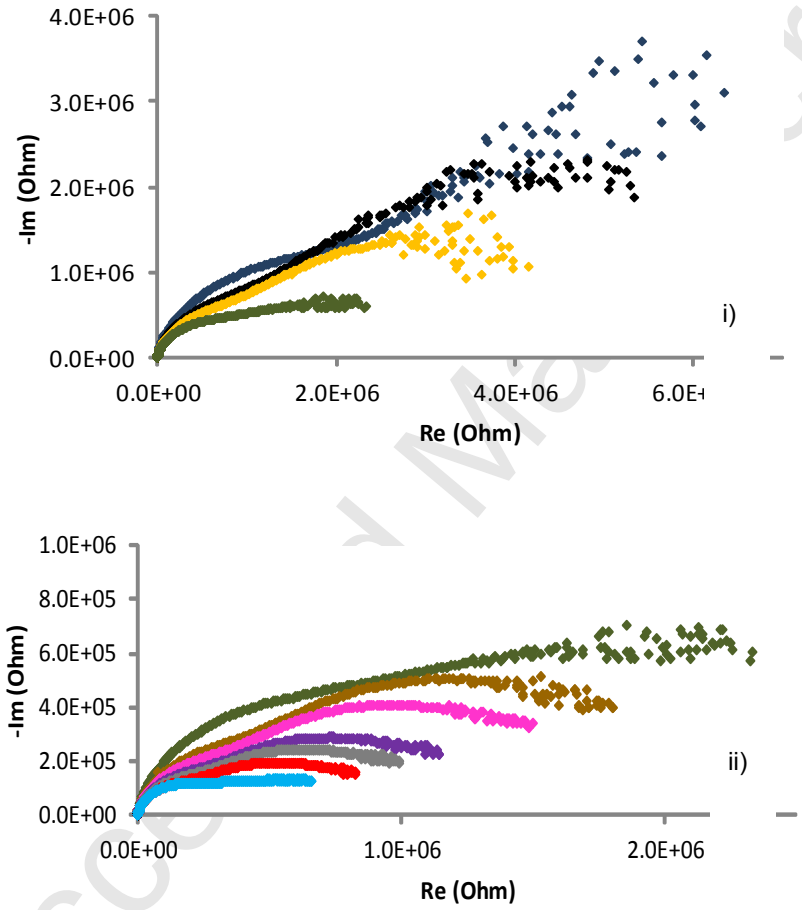

Figure 7 - Nyquist plot for sensor b at 30 and 40ºC, i) and ii) respectively (dark blue, black, orange, dark green, brown, rose, purple, grey, red and light blue, stand for 5, 15, 25, 30, 35, 40, 50, 70, 80 and 90% RH, in turn).

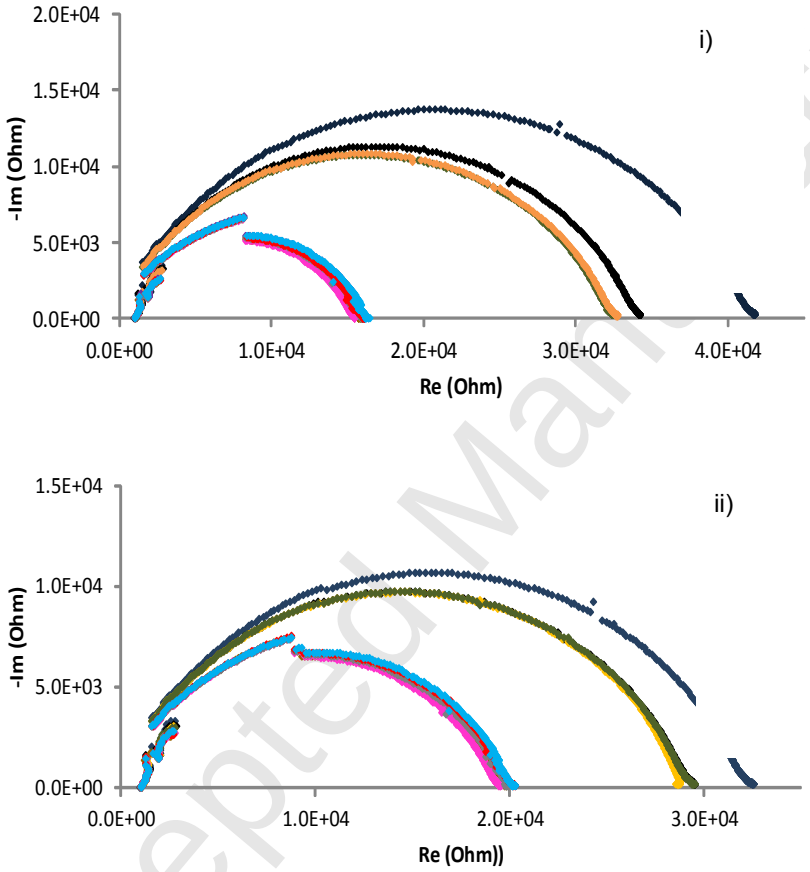

Figure 8 - Impedance change with RH, at 100 and 1 kHz, for sensor A, i) and ii), respectively, for all test temperatures (red 30ºC and blue 40ºC).

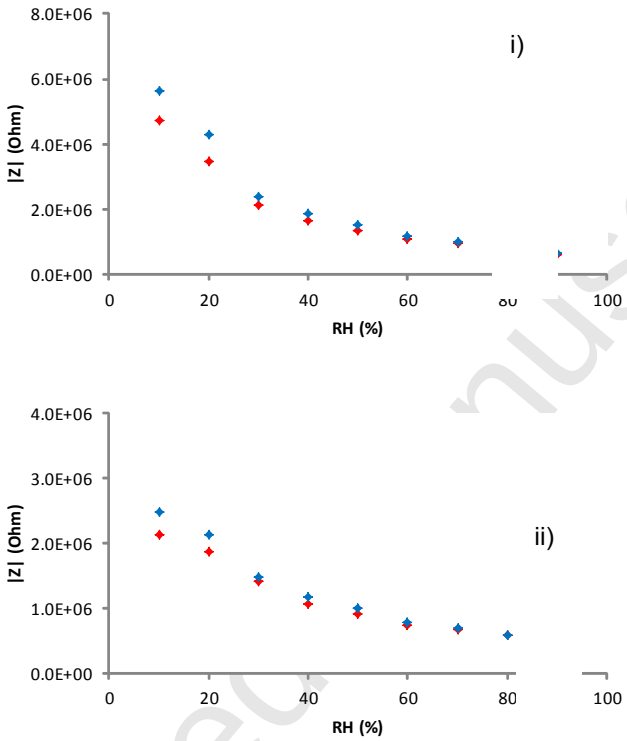

Figure 9 - Impedance change with RH, at 100 and 1 kHz, for sensor B, i) and ii), respectively, for all test temperatures (red 30ºC and blue 40ºC).

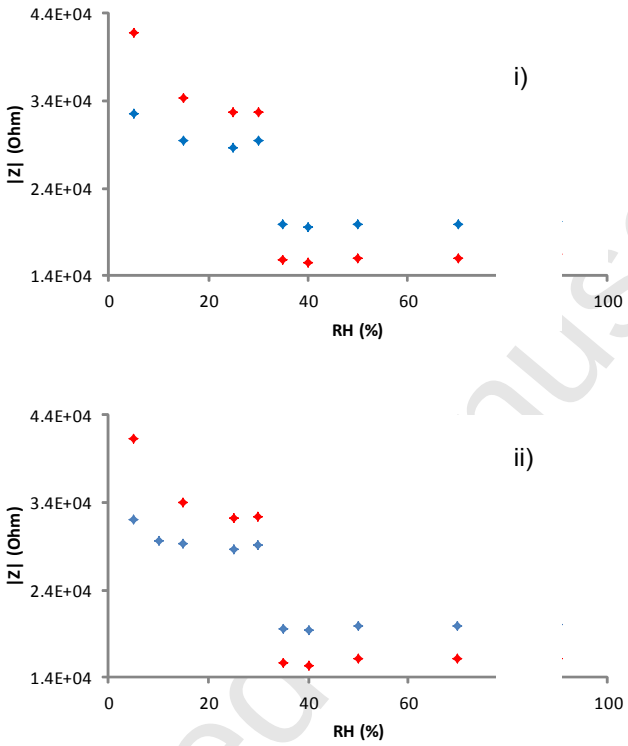

Figure 10 - Typical approach for modelling sensors electrical response to gases using model circuits (adapted from [30])

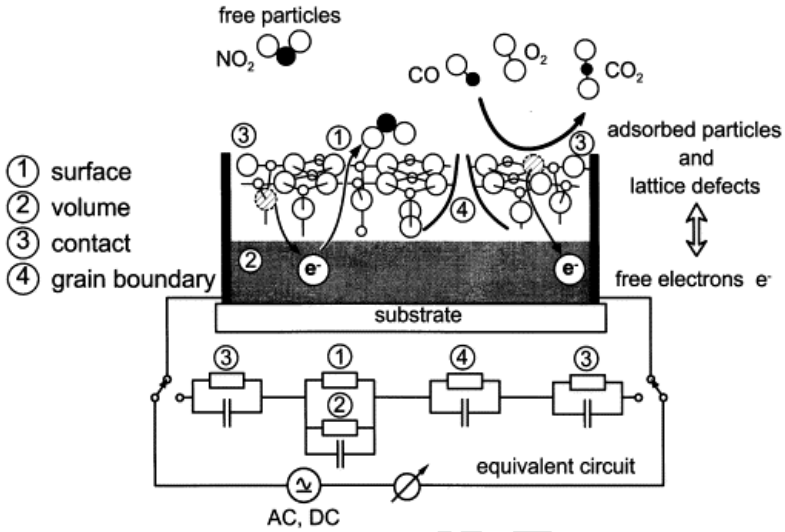

Figure 11 - Current equivalent circuit for the sensors.

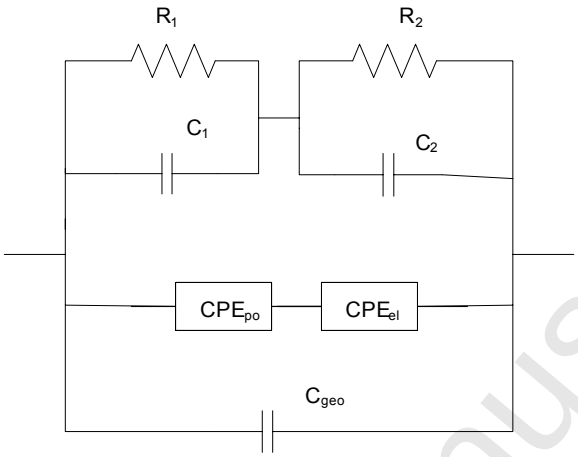

Figure 12 - Nyquist plots and best fitting for Sensor A, at 30ºC and 80% RH, at 30ºC and 30% RH and at 40ºC and 20% RH respectively i), ii), and iii) (red obtained spectra, blue fitted spectra).

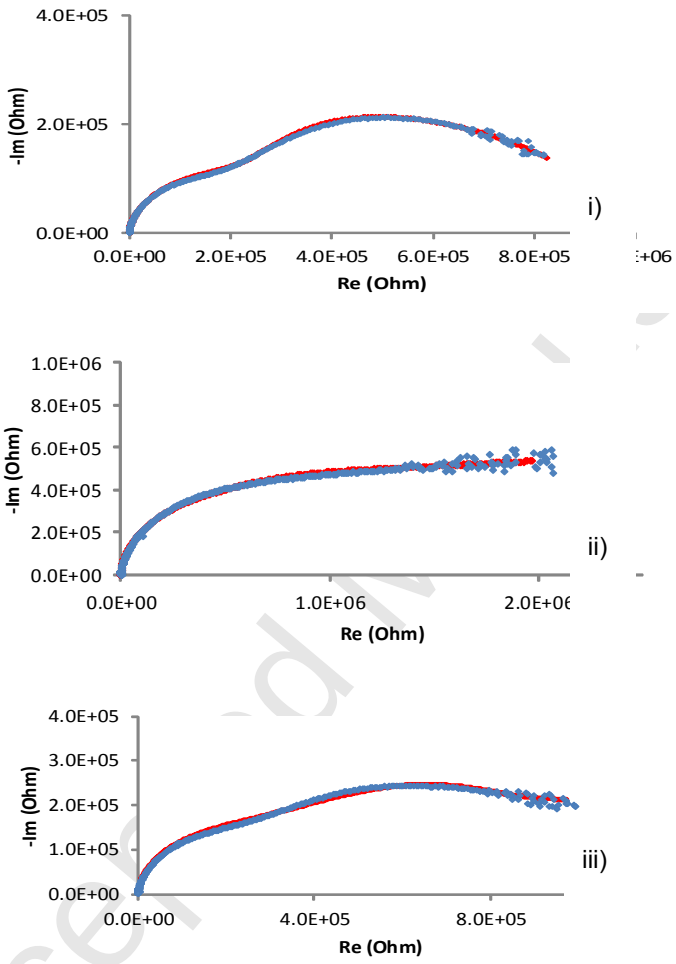

Figure 13 - Nyquist plots and best fitting for Sensor B, at 30ºC and 80% RH, at 30ºC and 30% RH and at 40ºC and 20% RH respectively i), ii), and iii) (red obtained spectra, blue fitted spectra).

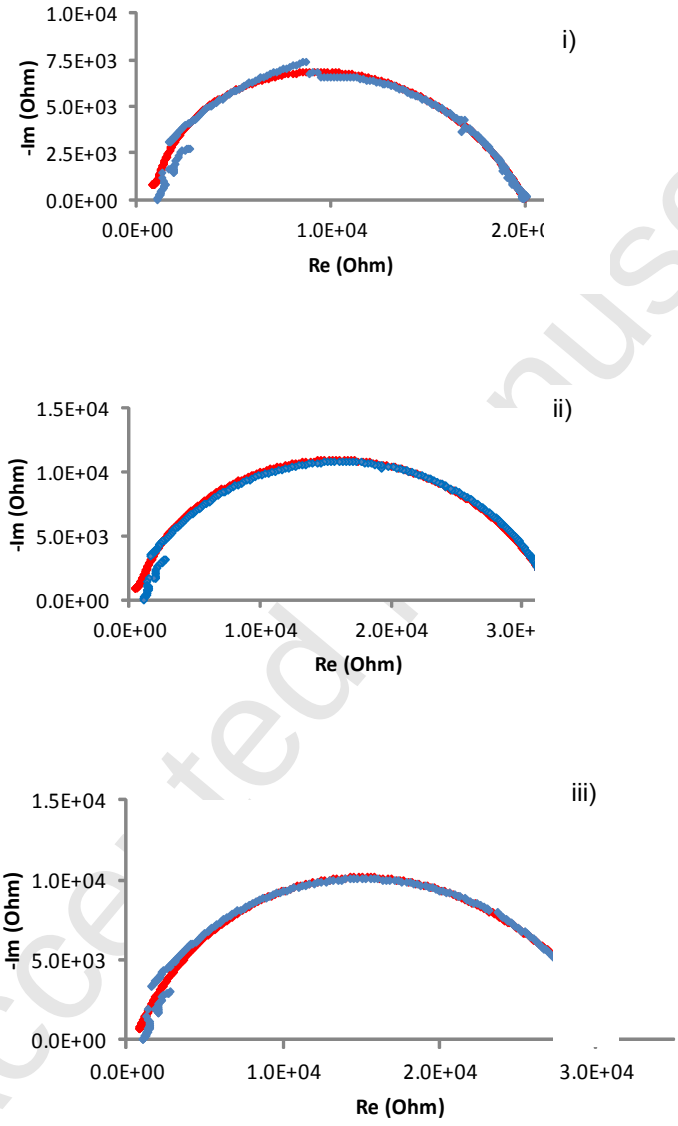

TiO_2:WO_3 composite humidity sensors doped with ZnO and CuO investigated by Impedance Spectroscopy

Pedro M. Faia[1,*], Emanuel L. Jesus[1] and Cristina S. Louro[2]

[1]CEMUC, Electrical and Computers Engineering Department, Faculty of Sciences and Technology of the University of Coimbra, Polo 2, Pinhal de Marrocos, 3030-290 Coimbra, Portugal

[2]CEMUC, Department of Mechanical Engineering, Faculty of Sciences and Technology of the University of Coimbra, Polo 2, Pinhal de Marrocos, 3030-788 Coimbra, Portugal

* corresponding author, email: faia@deec.uc.pt, Phone: +351-239-796200/62, Fax: +351-239796247

Abstract

For impedance type sensors based on semiconducting metal oxides, the overall conduction mechanisms strongly influence the magnitude and the direction of the sensor signal variation. For humidity in particular, the electronic/ionic charge transfer reactions that take place at the semiconductor surface can be used to monitor and control it. Along recent years, various mechanisms have been proposed to explain the variations of electrical response to humidity. With the study of composite materials we expect to obtain a better sensitivity of these sensors, when compared with the ones made out of only one metal oxide. This could be due to the fact that some of the positions initially occupied by the atoms of one of the metals are now occupied by atoms of the other metal: if a single covalent/ionic adsorption is decisive in the observed changes in the materials conductivity, then the electronegativity of the occupying metal atoms may be used to regulate the sensitivity. In this paper, TiO_2:WO_3 composite oxide bulk sensors, using 48.92 and 51.08% (w/w) of Titanium and of Tungsten atoms respectively, doped with the same proportions of Cooper and Zinc oxides (7%), were prepared by a conventional sintering method, and their dependence of their complex impedance spectra, measured in the range 100 Hz - 10 MHz, on the relative humidity (RH), operating temperature and on the measuring frequency is shown and explained.

HIGHLIGHTS

- Composite TiO_2:WO_3 were doped with ZnO or CuO and fabricated via a traditional forming and sintering process.
- The sensors structure was characterised using several techniques.
- The sensors electrical response to moisture was characterised by impedance spectroscopy.
- The sensors response was explained using the diverse electrical phenomena know to be present and the observed structure.
- We report a non-traditional approach to electrical circuit modelling of sensors overall response to moisture.